Rydberg electrons in intense fluctuating laser fields

G. Alber and B. Eggers

Fakultät für Physik, Albert-Ludwigs-Universität, D-79104 Freiburg im Breisgau, Germany
(Received 10 January 1997)

The influence of laser fluctuations on the optical excitation of Rydberg and continuum states close to a photoionization threshold is investigated within the framework of the phase diffusion model. Theoretical methods are developed for solving the relevant master equation of the atomic density operator which is averaged over the laser fluctuations. In the long-time limit this laser-induced excitation process exhibits non-exponential decay. This nonexponential time dependence reflects the fluctuation-induced diffusion of the Rydberg electron toward the ionization threshold. [S1050-2947(97)06006-X]

PACS number(s): 42.50.Ct, 42.50.Hz

I. INTRODUCTION

The dynamics of quantum systems under the influence of stochastic external forces is a major field of current physical interest [1]. An example which is of particular relevance in laser spectroscopy is the optical excitation of atomic or molecular systems by fluctuating laser fields. In recent years, research in this context has concentrated mainly on questions concerning the influence of laser fluctuations on resonant, possibly nonperturbative excitation of isolated energy eigenstates. By now the dynamics of these types of processes is fairly well understood [2]. However, still almost nothing is known about the influence of laser fluctuations on the optical excitation of atomic or molecular systems under conditions in which the level density of the resonantly excited states is large. A main intention of this paper is the exploration of this latter problem in Rydberg atoms.

Rydberg atoms are paradigms of physical systems with a high level density. The dynamics of a Rydberg electron in a laser field is dominated by two main characteristic properties, namely, (1) the localization of the electron-laser interaction in a region, which typically extends a few Bohr radii around the atomic nucleus only [3]; and (2) the large extension of the classically accessible region of space in which the dynamics of the Rydberg electron is dominated by the $1/r$ Coulomb potential of the ionic core [4]. According to property (1), which applies to electromagnetic fields of moderate intensities in the optical frequency regime, a Rydberg electron can be affected by a laser field only near the atomic nucleus. In contrast, the interaction of a Rydberg electron with an electromagnetic microwave field is completely different [5]. In this latter case the relevant excitation frequencies are typically of the same order of magnitude as the level spacings between adjacent Rydberg states. This implies that in the microwave regime photons can be absorbed by the Rydberg electron at any position within its classically accessible region of space. Property (2) implies a universal behavior of Rydberg systems [6]. Thus characteristic dynamical effects of atomic Rydberg systems can also be observed in more complex physical systems, such as molecules or clusters.

In this paper the influence of laser fluctuations on the optical one-photon excitation of atomic Rydberg states close to a photoionization threshold is investigated. Thereby we restrict ourselves to cases in which the laser fluctuations can be described within the framework of the phase diffusion model (PDM) [7]. This stochastic model describes the laser field of a realistic single mode laser with a well-stabilized amplitude. Furthermore, the laser intensities are assumed to be moderate in the sense that they are small in comparison with the atomic unit of intensity ($I = 1.40 \times 10^{17}$ W cm^{-2}), but still intense enough so that their influence on the atom cannot be described perturbatively. Therefore, in this intensity regime the phase fluctuations of the laser field will tend to destroy interferences between quantum-mechanical probability amplitudes which are associated with repeated returns of the Rydberg electron to the ionic core [8].

The main theoretical problem which has to be overcome is the nonperturbative treatment of the fluctuating laser field on the one hand, and the proper treatment of the threshold phenomena on the other hand, which originate from the infinitely many bound Rydberg states converging to the ionization threshold. In particular, we are interested in obtaining a dynamical description of the laser-induced excitation process which is also valid at very long interaction times. Due to inherent numerical inaccuracies, stochastic simulation methods are not suited for this purpose. In the following an alternative theoretical approach is used which takes advantage of special properties of the PDM. It is known that within the framework of the PDM a master equation can be derived for the atomic density operator which is averaged over the field fluctuations [9]. Master equations of this type are also studied in the context of the theory of continuous quantum measurement processes [10]. In the following it is shown that this master equation can be analyzed systematically with the help of quantum defect theory (QDT) [4,6]. Thereby all threshold phenomena which arise from the infinitely many bound Rydberg states and the adjacent electron continuum are taken into account properly. On the basis of this theoretical approach it will be shown that at sufficiently long interaction times the dynamics of the excited Rydberg electron is dominated by stochastic energy diffusion toward the photoionization threshold. The theoretical approach presented is well suited for investigating the resulting nonexponential features of the laser excitation process analytically.

The paper is organized as follows: In Sec. II, a theoretical description of one-photon excitation of Rydberg states close to a photoionization threshold is developed. With the help of

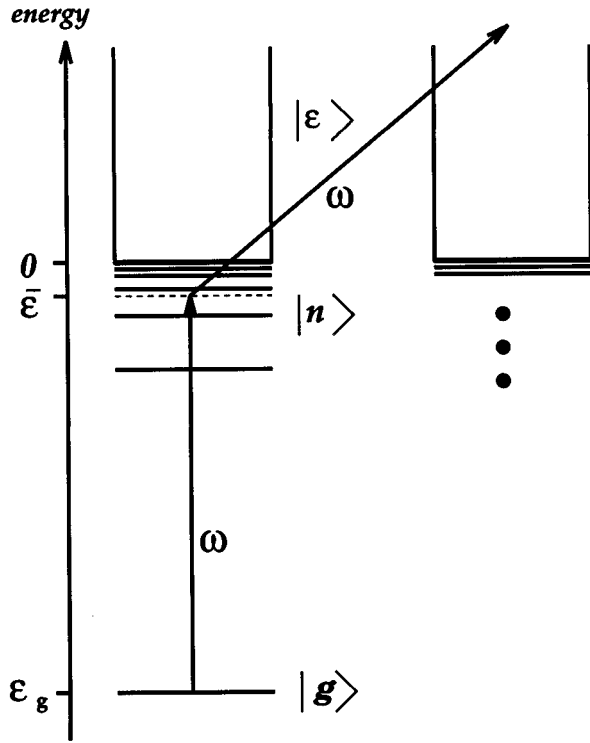<u>56</u>   820   © 1997 The American Physical Society

FIG. 1. Schematic representation of the excitation process.

QDT a Fourier representation of the (averaged) atomic density operator is developed. This representation is useful for numerical, highly accurate calculations of relevant atomic observables which are averaged over the phase fluctuations of the laser field. Furthermore, it is a convenient starting point for the derivation of analytical results on the long-time dynamics of the excitation process. This section concentrates on the presentation of the main ideas and main theoretical results. Details of mathematical derivations can be found in Appendices A, B, and C. Numerical examples which exhibit the characteristic physical effects originating from the phase fluctuations of the laser field are presented in Sec. III. A short summary and conclusions are given in Sec. IV.

II. THEORETICAL DESCRIPTION

In this section a theoretical description of one-photon excitation of Rydberg states by a laser field with fluctuating phase is developed. Mathematical details of derivations are postponed to Appendixes A, B, and C.

Let us consider one photon excitation of Rydberg and continuum states close to a photoionization threshold, as shown schematically in Fig. 1. Thereby these Rydberg and continuum states are excited from an initially prepared energetically low-lying bound state $|g\rangle$ with energy ϵ_g. In the dipole and rotating-wave approximations, this excitation process is characterized by the Hamiltonian

$$H(\Phi(t)) = \epsilon_g |g\rangle\langle g| + \sum_n \epsilon_n |n\rangle\langle n|$$

$$- \sum_n (|n\rangle\langle g| \langle n|\mathbf{d}|g\rangle \cdot \mathbf{E}_0 e^{i\Phi(t)} e^{-i\omega t} + \text{H.c.}). \quad (1)$$

Thereby the index n refers to Rydberg and continuum states. Atomic units are used with $e = \hbar = m_e = 1$. In Eq. (1) it is

assumed that the exciting fluctuating cw-laser field of frequency ω can be described by the classical electric field

$$\mathbf{E}(t) = \mathbf{E}_0 e^{i\Phi(t)} e^{-i\omega t} + \text{c.c.}, \quad (2)$$

whose amplitude is well stabilized and whose phase is fluctuating. For near-ideal single-mode laser fields to a good degree of approximation, these phase fluctuations can be described by the PDM [7], in which the stochastic phase variation $\Phi(t)$ is given by a real-valued Wiener process with $M\, d\Phi(t) = 0$ and $[d\Phi(t)]^2 = 2b\, dt$ (M denotes averaging over the statistical ensemble). The energies of the excited Rydberg and continuum states are denoted ϵ_n, and $\mathbf{d}$ is the atomic dipole operator. Within the framework of QDT [4] and the one-channel approximation, the excited states are characterized by a complex quantum defect $\mu = \alpha + i\beta$. The real part of this quantum defect defines the energies of the bound states in the absence of the laser field, i.e., $\epsilon_n = -1/[2(n-\alpha)^2]$. The imaginary part β describes effects arising from photon absorption from the highly excited states close to threshold to continuum states well above threshold. As long as the laser intensity I is small on the atomic scale, i.e., $I \ll I_0 = 1.40 \times 10^{17}$ W cm^{-2}, in the optical frequency regime this photon absorption process can be described perturbatively with [11]

$$\beta = \langle \epsilon = \omega |\mathbf{d} \cdot \mathbf{E}_0| \epsilon = 0\rangle. \quad (3)$$

Such a perturbative treatment is valid as long as the oscillation amplitude $\alpha_{\text{osc}} = |\mathbf{E}_0| \omega^{-2}$ of an electron in the laser field is significantly smaller than the Bohr radius which defines the characteristic length scale of atomic quantum phenomena. The matrix element of Eq. (3) can be estimated semiclassically, for example, with the help of the Bohr correspondence principle. Thus it is found [12] that

$$\beta = 6^{2/3}\Gamma(2/3)\omega^{-5/3}|\mathbf{E}_0|/(2\pi\sqrt{3}). \quad (4)$$

The $\omega^{-5/3}$ dependence of this semiclassical result reflects the fact that the dominant contribution to the matrix element of Eq. (3) originates from a spatial region around the atomic nucleus with a typical size of the order of $r_c \approx \omega^{-2/3}$. This characteristic size r_c is determined by the distance a classical electron can depart from a singly charged nucleus during the relevant photon absorption time $t_{\text{photon}} = \omega^{-1}$, while it is moving on a parabolic, classical Kepler orbit of angular momentum zero. Thus in the optical frequency regime this leads to the well-known conclusion [3] that the photon absorption process takes place in a region extending only a few Bohr radii around the atomic nucleus, a region which is small in comparison with the extension of highly excited Rydberg states of large eccentricity.

In order to describe nonperturbative aspects of the dynamics of the laser excitation process, one has to solve the stochastic linear Schrödinger equation with Hamiltonian (1), and has to average observables of interest over the laser fluctuations. In this context straightforward, numerical stochastic simulation approaches [13] offer the general advantage that they are applicable to any types of laser fluctuations. However, this way it is difficult to obtain numerically reliable results for threshold phenomena which originate from the infinitely many Rydberg and continuum states close to

threshold. In particular, due to unavoidable numerical inaccuracies it is very difficult to investigate long time phenomena which are direct consequences of these threshold effects. Therefore, in this paper an alternative theoretical approach is used which takes advantage of special properties of the PDM, and which allows the long-time behavior to be evaluated accurately. It is well known [9] that the mean values

$$\rho_{nn'}(t) = \rho^*_{n'n}(t) = M\langle n|\psi(t)\rangle\langle\psi(t)|n'\rangle,$$

$$\rho_{ng}(t) = \rho^*_{gn}(t) = Me^{-i\Phi(t)}\langle n|\psi(t)\rangle\langle\psi(t)|g\rangle, \quad (5)$$

$$\rho_{gg}(t) = M|\langle g|\psi(t)\rangle|^2$$

can be combined to form a density operator $\rho(t)$. Thereby $|\psi(t)\rangle$ denotes the atomic state which is associated with a single realization of the fluctuating laser field. The density operator $\rho(t)$ fulfills the master equation [9]

$$\frac{d}{dt}\rho(t) = -i[H_{\text{mod}},\rho(t)] + \frac{1}{2}\{[L,\rho(t)L^\dagger] + [L\rho(t),L^\dagger]\}. \quad (6)$$

The Hamiltonian $H_{\text{mod}} \equiv H(\Phi(t)\equiv 0)$ describes laser-induced excitation in the absence of phase fluctuations. The destruction of coherence due to the laser fluctuations is described by the Lindblad operator

$$L = \sqrt{2b}|g\rangle\langle g|. \quad (7)$$

Master equations of this type are also of general interest as phenomenological descriptions of deterministic excitation processes in the presence of continuous measurement of the initial state $|g\rangle$ [10]. In this context $1/b$ can be interpreted as the mean time between subsequent measurements. So far master equations of the form of Eq. (6) have been studied only in cases in which the number of resonantly coupled states is small. In the following it will be shown that these master equations are also useful starting points for investigating nonperturbative laser-induced threshold phenomena of Rydberg systems.

For the subsequent treatment it is convenient to represent the formal solution of Eq. (6) as a sum over all possible quantum jumps which are induced by the Lindblad operator L [14], i.e., $\rho(t) = \Sigma^\infty_{N=0}\rho^{(N)}(t)$, with

$$\rho^{(N)}(t) = \int_0^t dt_N \cdots \int_0^{t_2} dt_1 |\psi(t|t_N,\ldots,t_1)\rangle$$

$$\times\langle\psi(t|t_N,\ldots,t_1)|$$

being a mixture of the pure states

$$|\psi(t|t_N,\ldots,t_1)\rangle = e^{-i\bar{H}(t-t_N)}L\cdots Le^{-i\bar{H}t_1}|\psi(0)\rangle. \quad (8)$$

The effective Hamiltonian

$$\bar{H} = H_{\text{mod}} - iL^\dagger L/2 \quad (9)$$

describes the deterministic time evolution between successive quantum jumps which take place at the random jump times $t_1,t_2,\ldots,t_N$. In terms of the Laplace-transformed quantities

$$A_{ij}(z) = \int_0^\infty dt\ e^{izt}\langle i|e^{-i\bar{H}t}|g\rangle\langle j|e^{-i\bar{H}t}|g\rangle^*, \quad (10)$$

with $i,j \in \{n,g\}$, this decomposition of the formal solution of Eq. (6) yields

$$\rho_{ij}(t) = \frac{1}{2\pi}\int_{-\infty+i0}^{\infty+i0} dz\ e^{-izt}A_{ij}(z)\sum_{N=0}^\infty [2bA_{gg}(z)]^N$$

$$= \frac{1}{2\pi}\int_{-\infty+i0}^{\infty+i0} dz\ e^{-izt}A_{ij}(z)[1-2bA_{gg}(z)]^{-1}. \quad (11)$$

As $|2bA_{gg}(z)| < 1$, Eq. (11) represents a convergent geometric series. Thus the main problem is the evaluation of the characteristic kernels $A_{ij}(z)$. This can be achieved with the help of QDT. Thereby it is possible to include effects of the infinitely many bound Rydberg and continuum states properly. It is shown in detail in Appendix A that

$$A_{gg}(z) = U(z) + U^*(-z), \quad (12)$$

with

$$U(z) = \left\{ -C_2(z) + C_4(z) + i\sum_{\text{Re}\bar\epsilon_n<0}\left[1 - \frac{d}{dz_1}\Sigma^*(z_1-z)\right]^{-1} \right.$$

$$\left. \times [z_1 - \bar\epsilon + ib - \Sigma(z_1)]^{-1}\big|_{z_1=z+\bar\epsilon^*_n} \right\}\Theta(z),$$

$$C_2(z) = \frac{1}{2\pi(z+2ib)}\ln\frac{z-\bar\epsilon+i(b+\gamma/2)}{-\bar\epsilon+i(\gamma/2-b)},$$

$$C_4(z) = \frac{1}{2\pi[z+i(\gamma+2b)]}\ln\frac{z-\bar\epsilon+i(\gamma/2+b)}{-\bar\epsilon-i(\gamma/2+b)}. \quad (13)$$

Thereby the branches of the logarithmic functions have to be chosen in agreement with the definitions of Eq. (A5) of Appendix A. Analogous expressions are obtained for the (averaged) coherences of the Rydberg and continuum states $A_{nn'}(z)$ and $A_{\epsilon\epsilon'}(z)$. Their explicit form is given in Eq. (A7) of Appendix A.

The sum of Eq. (13) extends over all dressed states with energies $\tilde\epsilon_n$ which are determined by the condition

$$\tilde\epsilon_n - \bar\epsilon + ib - \Sigma(\tilde\epsilon_n) = 0. \quad (14)$$

The quantity $\Sigma(z)$ denotes the resonant part of the self-energy of state $|g\rangle$, and is defined by [11]

$$\Sigma(z) = \sum_n \frac{|\langle n|\mathbf{d}\cdot\mathbf{E}_0|g\rangle|^2}{z-\epsilon_n}$$

$$= -i\frac{\gamma}{2} - \frac{i\gamma\chi}{e^{-i2\pi(-2z)^{-1/2}}-\chi}. \quad (15)$$

It is characterized by the laser-induced depletion rate

$$\gamma = 2\pi|\langle\epsilon=0|\mathbf{d}\cdot\mathbf{E}_0|g\rangle|^2$$

of the initial state $|g\rangle$ and the scattering matrix element [11]

$$\chi = e^{i2\pi\mu},$$

which describes all effects arising from scattering of the Rydberg electron by the ionic core and photon absorption.

Equation (13) is a major result of this paper. Combined with Eq. (11) it is useful for numerically accurate calculations of relevant atomic observables which are averaged over the laser fluctuations. Furthermore, it is a convenient starting point for the derivation of analytical results which describe the long-time dynamics of the laser-induced excitation process. This long-time dynamics is dominated by the behavior of $A_{gg}(z)$ in a small neighborhood of its branch point at $z=0$ in the complex z plane [15].

In order to discuss this long-time dynamics, let us neglect ionization from highly excited Rydberg states to continuum states well above threshold, i.e., $\beta=0$. Effects of photon absorption from the excited Rydberg states will be taken into account in the numerical examples presented in Sec. III. It is shown in Appendix B that for sufficiently small values of z two dynamical regimes can be distinguished:

(1) $|z| \ll 1/t_c$:

If the values of z are much smaller than the inverse characteristic time

$$t_c = \frac{4\pi}{\gamma b \sqrt{27}}\left[\frac{(\bar{\epsilon}^2 + 3(b^2+\gamma^2/4)/4)^{3/2}}{\bar{\epsilon}^2 + b^2 + \gamma^2/4}\right]^{1/2}, \quad (16)$$

the asymptotic relation

$$A_{gg}(z) = U(z=0) - \frac{2\pi}{12\sqrt{3}b^2}\left[\frac{b\gamma}{\pi(\bar{\epsilon}^2+b^2+\gamma^2/4)}\right]^{1/3}$$
$$\times e^{-i\pi/3}z^{2/3} + O(z) \quad (17)$$

is found with

$$U(z=0) = \frac{1}{2b}\left[1 - \frac{\gamma}{\gamma+2b}\frac{\varphi}{\pi}\right], \quad (18)$$

and with $-\bar{\epsilon} + i(b+\gamma/2) = re^{i\varphi}$ $(0 < \varphi < \pi)$.

(2) $-\bar{\epsilon} \gg b$, $1/t_c < |z|$:

In this case Rydberg states well below threshold are excited, and one obtains

$$A_{gg}(z) = \frac{1}{2b} - \frac{e^{-i\pi/4}}{8b^2}\sqrt{2b\gamma T_{\bar{\epsilon}}}\,z^{1/2} + O(z). \quad (19)$$

The mean classical orbit time of the excited Rydberg states is denoted $T_{\bar{\epsilon}} = 2\pi(-2\bar{\epsilon})^{-3/2}$.

These asymptotic relations show explicitly that $A_{gg}(z)$ does not have poles in a small neighborhood of its branch point at $z=0$. According to Eq. (11) the time evolution of the averaged atomic density matrix elements can be evaluated by inverting the Laplace transform with the help of contour integration in the complex z plane. Thereby the poles of the integrand with negative imaginary parts give rise to exponentially decaying terms. Any nonexponential contribution arises from contour integration along the branch cut which, according to Eqs. (17) and (19), starts at $z=0$. This cut contribution dominates the long-time behavior, and is given by

$$\rho_{ij}(t) = -\frac{1}{\pi}\text{Re}\left\{i\int_0^\infty dy\ e^{-yt}A_{ij}(e^{-i\pi/2}y)\right.$$
$$\left.\times[1 - 2bA_{gg}(e^{-i\pi/2}y)]^{-1}\right\}. \quad (20)$$

Equation (20) indicates that it is only the immediate neighborhood of the branch point at $z=0$ which contributes significantly in the limit $t \to \infty$. Inserting the asymptotic expressions of Eqs. (17) and (19) into Eq. (20) in the limit of long interaction times t, the following asymptotic decay laws are obtained for $\rho_{gg}(t)$:

(1) $t \gg t_c$:

$$\rho_{gg}(t) = \frac{(\gamma+2b)^2}{(2b\gamma\varphi/\pi)^2}\left[\frac{\gamma b\Gamma^3(5/3)t^{-5}}{27\pi(\bar{\epsilon}^2+b^2+\gamma^2/4)}\right]^{1/3}. \quad (21)$$

(2) $-\bar{\epsilon} \gg b$, $t < t_c$:

$$\rho_{gg}(t) = \frac{2}{\pi}\Gamma(1/2)[2b\gamma T_{\bar{\epsilon}}]^{-1/2}t^{-1/2}. \quad (22)$$

Thereby $\Gamma(x) = \int_0^\infty du\ e^{-u}u^{x-1}$ denotes the gamma function [16]. Analogous expressions can be found for the other density-matrix elements.

Equations (21) and (22) together with Eqs. (11), (13,) and (A7) are the main results of this paper. Within the phase diffusion model they describe the influence of laser fluctuations on nonperturbative laser excitation in the energy region close to the photoionization threshold. Equations (21) and (22) imply that for sufficiently long interaction times between the Rydberg atom and the laser field, the initial state exhibits a nonexponential decay as long as ionization from highly excited Rydberg states to continuum states well above threshold is negligible. In particular, this conclusion also holds for resonant laser excitation of Rydberg states well below threshold, in which the field-induced depletion rate γ and the laser bandwidth b are much smaller than the level spacing between adjacent Rydberg states, and in which at first sight a two-level approximation should be valid. Within the framework of such a two-level approximation the initial state probability $\rho_{gg}(t)$ tends to the stationary value 0.5 in the long-time limit. Physically speaking the nonexponential, asymptotic time evolution predicted by Eqs. (21) and (22) reflects diffusion of the excited Rydberg electron to higher-lying energy eigenstates close to the photoionization threshold. The dynamics of this stochastic energy diffusion toward threshold cannot be described properly within the framework of a two- or few-level approximation. It is the presence of the infinitely many bound states converging to the photoionization threshold which dominates this process. Eq. (21) is valid irrespective of whether energy eigenstates below or above threshold are excited by the laser field. Thus for interaction times $t \gg t_c$ a nonexponential depletion of the initial state $|g\rangle$ is predicted even if continuum states above threshold are excited dominantly. However, well above threshold, i.e., for $\bar{\epsilon} \gg \sqrt{b^2+\gamma^2/2}$, the critical time t_c of Eq. (16) tends to infinity.
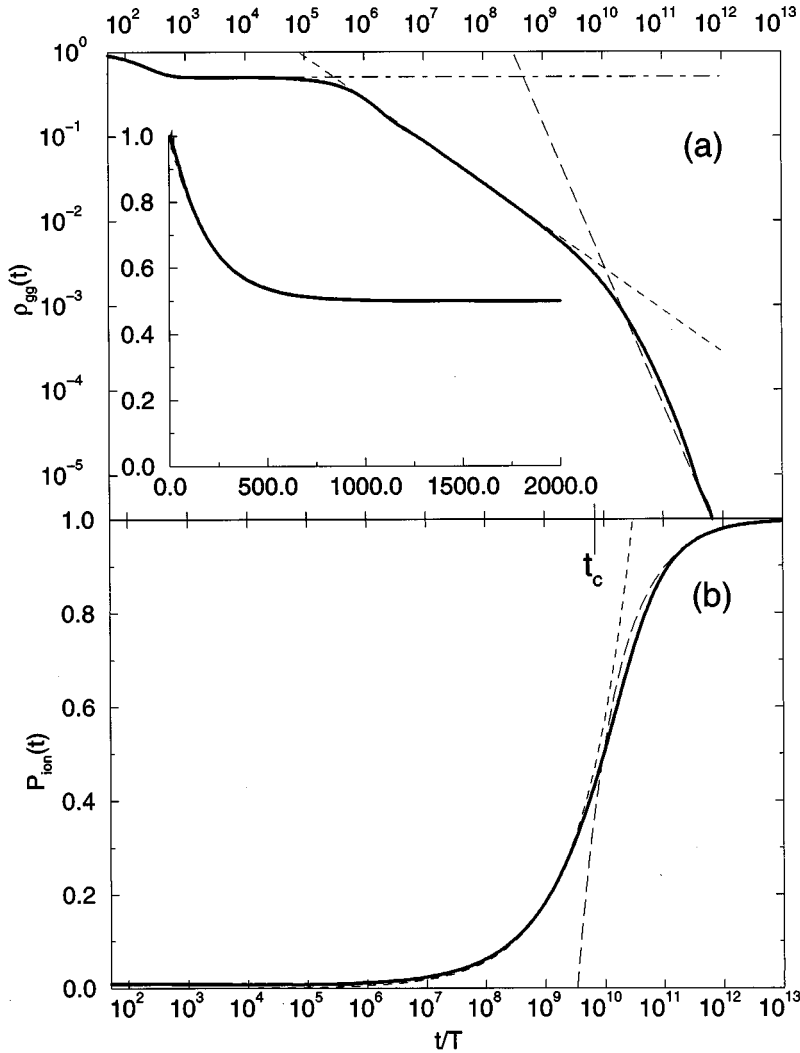
FIG. 2. Initial-state probability $\rho_{gg}(t)$ (a) and ionization probability $P_{\mathrm{ion}}(t)$ (b) as a function of interaction time t in units of the mean classical orbit time T, with $\bar{\nu}=(-2\bar{\epsilon})^{-1/2}=80$, $\gamma T=10^{-4}$ and $bT=0.08$. Various approximate time dependences are also indicated, namely, (a) $\rho_{gg}(t)=(1+e^{-2Rt})/2$, with $R=2\gamma/bT$ (long dashed, short dashed), Eq. (22) (short dashed), and Eq. (21) (long dashed); and (b) Eqs. (23) (short dashed) and (24) (long dashed).

III. NUMERICAL RESULTS

In the subsequent numerical examples the mean initial state and ionization probabilites $\rho_{gg}(t)$ and $P_{\mathrm{ion}}(t)$ $=\int_0^\infty d\epsilon\, \rho_{\epsilon\epsilon}(t)$, as obtained from Eqs. (11), (13), and (A7), are compared with the corresponding analytical predictions of Eqs. (21) and (22). The parameters used refer to optical excitation of hydrogen from the initial state $|g\rangle=|2s\rangle$ by linearly polarized laser light. In these numerical results, ionization by absorption of optical photons from the highly excited Rydberg states is taken into account by the imaginary quantum defect $\mu=i\beta$. In agreement with the semiclassical estimate of Eq. (4), it is assumed that $\beta=0.00375\gamma$.

In Fig. 2 the laser-induced depletion rate γ and the bandwidth b are small in comparison with the mean level spacing of the excited Rydberg state, i.e., $\gamma T_{\bar{\epsilon}}\ll bT_{\bar{\epsilon}}\ll 1$. Thus, seemingly, only one Rydberg state is excited resonantly by the fluctuating laser field, and it is expected that this case can be described adequately in the two-level approximation. In Fig. 2(a), well-known characteristic features of resonant two-level excitation by a fluctuating laser field are apparent [2]. As $b\gg\gamma$, initially $\rho_{gg}(t)$ decays exponentially with rate $R=2\gamma/(bT_{\bar{\epsilon}})$, and reaches the statistical equilibrium value of 0.5 [9]. In particular, the decay rate R is inversely proportional to the bandwidth of the laser field. Within the two-level limit this particular dependence implies that for fixed

interaction time t the initial-state probability tends to the value 1 in the limit $b\to\infty$. The appearance of this quantum Zeno effect [17] is a plausible consequence of the formal similarity between Eq. (6) and master equations which describe laser excitation processes in the presence of continuous measurement of an initial state [10]. In this analogy the parameter $1/b$ corresponds to the mean time between subsequent measurements. However, for longer interaction times the initial-state probability exhibits a nonexponential decay which to a good degree of approximation is described by Eq. (22). The physical reason for this nonexponential decay is stochastic energy diffusion of the excited Rydberg states toward the photoionization threshold which is brought about by the fluctuations of the laser field. This physical picture is consistent with the corresponding increase of the ionization probability in Fig. 2(b). From Eqs. (11) and (A7) it can be shown that for these interaction times the ionization probability is approximately given by

$$P_{\mathrm{ion}}(t)=\frac{4\varphi\sqrt{2b\gamma t/T_{\bar{\epsilon}}}}{\pi^{3/2}(\gamma+2b)}. \tag{23}$$

It is worth mentioning that the nonexponential decay described by Eq. (22) can also be derived under the assumption of an equidistant level spacing between the excited Rydberg
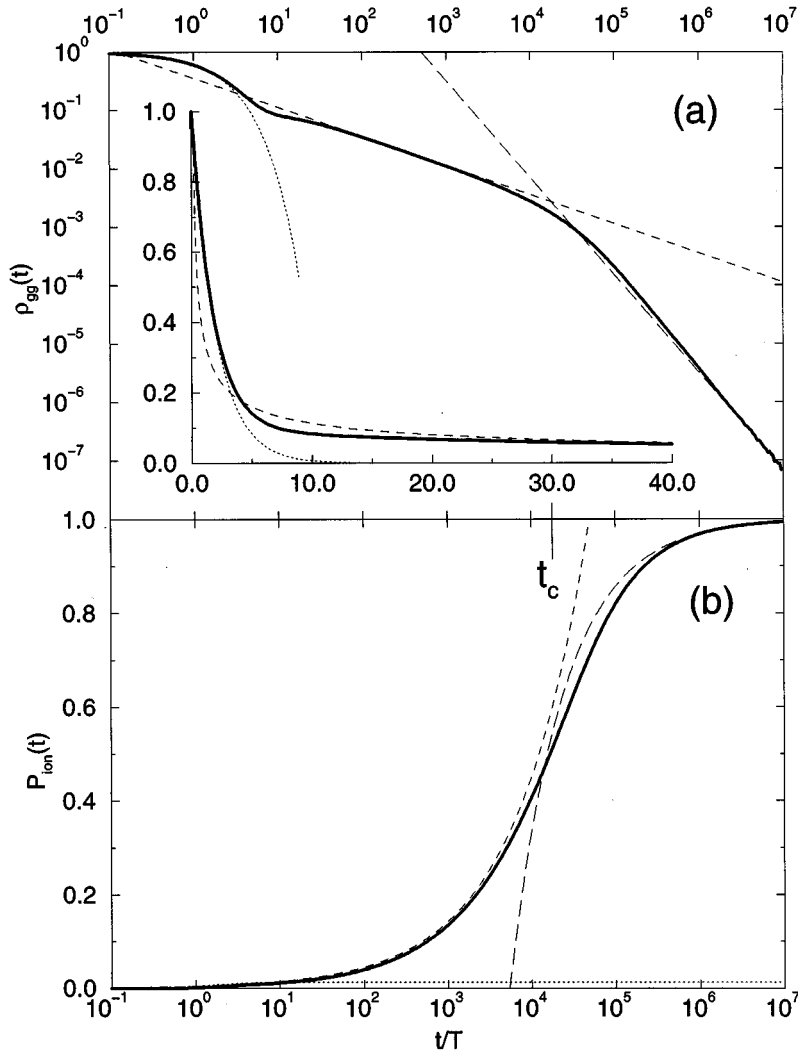
FIG. 3. Initial-state probability $\rho_{gg}(t)$ (a) and ionization probability $P_{\text{ion}}(t)$ (b) as a function of interaction time t in units of the mean classical orbit time T with $\bar{\nu} = (-2\bar{\epsilon})^{-1/2} = 80$, $\gamma T = 0.5$ and $bT = 10$. Various approximate time dependences are also indicated, namely, (a) $\rho_{gg}(t) = e^{-\gamma t}$ (dotted), Eq. (22) (short dashed), and Eq. (21) (long dashed); and (b) Eqs. (25) (dotted), (23) (short dashed), and (24) (long dashed).

states. This indicates that for these interaction times the Rydberg electron has been diffusing over a small energy interval only over which the level spacing of the Rydberg states is approximately equidistant. For interaction times larger than the characteristic time t_c of Eq. (16), finally the nonexponential decay crosses over to a $t^{-5/3}$-decay law, as predicted by Eq. (21). At these long interaction times the stochastic energy diffusion of the Rydberg electron has reached the photoionization threshold, and the ionization probability increases significantly. With the help of Eqs. (20) and (B2) it can be shown that, for $t > t_c$, the ionization probability is given approximately by

$$P_{\text{ion}}(t) = 1 - \frac{\pi \Gamma(2/3)(\gamma + 2b)}{6 b \gamma \varphi} \left[\frac{\gamma b}{\pi(\bar{\epsilon}^2 + b^2 + \gamma^2/4)} \right]^{1/3} t^{-2/3}. \tag{24}$$

The characteristic long-time behavior which has been derived in Sec. II under the assumption of negligible photon absorption from the excited Rydberg states is clearly visible in Fig. 2, as for the interaction times considered photon absorption from the Rydberg states is still negligible, i.e., $\Gamma_{\bar{\epsilon}} t = 4\pi\beta/T_{\bar{\epsilon}} < 1$ ($\Gamma_{\bar{\epsilon}}$ denotes the laser-induced ionization rate of Rydberg states with energy $\bar{\epsilon}$).

In Fig. 3 the bandwidth b is much larger than the mean

level spacing between the excited Rydberg states, but $\gamma T_{\bar{\epsilon}} < 1$. Now even the initial stage of this excitation process can no longer be described within the framework of a two-level approximation. As apparent from Fig. 3, initially state $|g\rangle$ decays with rate γ. Physically this might be traced back to the large bandwidth of the laser field which tends to "smear out" the discrete Rydberg states. As can be shown from Eqs. (11) and (A7), this initial stage of the ionization process is approximately described by the relation

$$P_{\text{ion}}(t) = \frac{\varphi}{\pi}(1 - e^{-\gamma t}), \tag{25}$$

with φ being defined in Eq. (18). At larger interaction times the Rydberg electron starts to diffuse to higher-energy eigenstates closer to the photoionization threshold. Thus the decay of the initial state becomes nonexponential, and is described approximately by Eq. (22). At the critical time t_c, finally, the diffusing Rydberg electron has already reached the photoionization threshold. Therefore the ionization probability rises significantly and the decay of the initial state crosses over to the $t^{-5/3}$-decay law predicted by Eq. (21). Similar to Fig. 2, all these asymptotic effects take place long before photon absorption from the highly excited states becomes important.
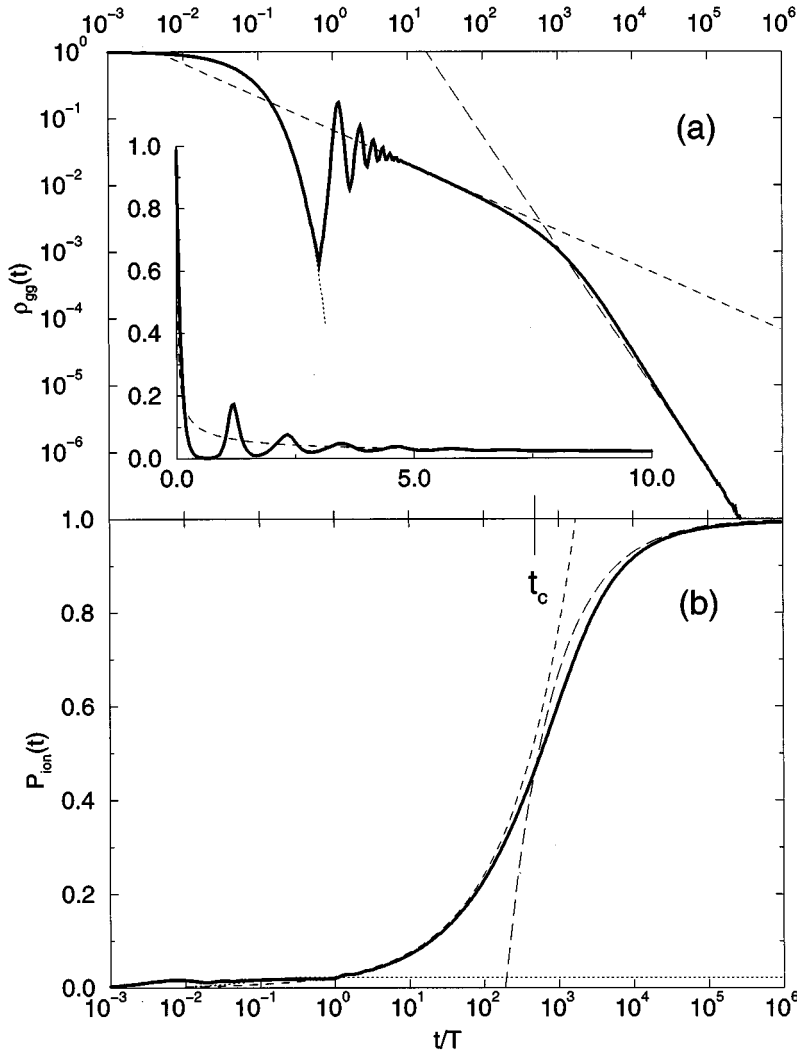
FIG. 4. Initial-state probability $\rho_{gg}(t)$ (a) and ionization probability $P_{\text{ion}}(t)$ (b) as a function of interaction time t in units of the mean classical orbit time T with $\overline{\nu}=(-2\overline{\epsilon})^{-1/2}=80$, $\gamma T_{\overline{\epsilon}}=12$ and $bT_{\overline{\epsilon}}=12$. Various approximate time dependences are also indicated, namely, (a) $\rho_{gg}(t)=e^{-\gamma t}$ (dotted), Eq. (22) (short dashed), and Eq. (21) (long dashed); and (b) Eqs. (25) (dotted), (23) (short dashed), and (24) (long dashed).

In Fig. 4 both the bandwidth b of the laser field and the field-induced depletion rate γ are larger than the mean level spacing of the excited Rydberg states, i.e., $bT_{\overline{\epsilon}}, \gamma T_{\overline{\epsilon}} \gg 1$. Thus an electronic Rydberg wave packet is prepared by power broadening [11]. This wave packet evolves under the combined influence of the Coulomb potential of the ionic core and the fluctuating laser field. Whenever it returns to the core region it is scattered resonantly by the laser field. The maxima near multiples of the mean classical orbit time $T_{\overline{\epsilon}}$ result from laser-induced stimulated transitions of this wave packet to the initial state at one of the wave packet's returns to the ionic core. In this example the bandwidth of the fluctuating laser field is large, i.e., $bT_{\overline{\epsilon}} \gg 1$. This implies that coherent effects arising from laser-induced resonant scattering during one of the wave packet's intermediate returns to the core region, which typically lead to scattering-induced time delays, are not seen. The absence of these effects originates from the fluctuation-induced destruction of all coherences associated with physical processes which occur at repeated returns of the electronic Rydberg wave packet to the ionic core. At sufficiently large interaction times, at which $e^{-\gamma t} < 1/\sqrt{2bt\gamma T_{\overline{\epsilon}}}$, the recurrence peaks disappear and the initial state probability exhibits the characteristic nonexponential decay described by Eq. (22). At these interaction times the dynamics of the excited Rydberg electron starts to be dominated by stochastic energy diffusion, and the coher-

ent dynamics of the electronic wave packet is destroyed. This stochastic energy diffusion of the Rydberg electron leads to an increase of the ionization probability which is described approximately by Eq. (23). At interaction times $t > t_c$ the energy diffusion of the Rydberg electron has reached the photoionization threshold. Thus the initial state decays according to the decay law of Eq. (21), and the photoionization probability is described approximately by Eq. (24).

In Fig. 5, Rydberg and continuum states very close to threshold are excited. The bandwidth of the laser field is large, i.e., $b \gg \gamma$. Thus the phase fluctuations of the laser field dominate the dynamics of the excitation process. Initially the initial state decays with rate γ. Physically speaking this is caused by the large bandwidth of the laser field which tends to smooth out the excited, discrete energy levels, so that the Rydberg electron behaves as if it were excited into a flat continuum. Initially the ionization probabilty increases exponentially and reaches a metastable equilibrium value of approximately 0.5. As the initial-state probability is very small, this implies that with a probability of 0.5 the Rydberg electron is either in a bound Rydberg state or in a continuum state. This initial stage of the ionization process is described approximately by Eq. (25). Furthermore, from Eqs. (11) and (B1) it is straightforward to show that for interaction times $|\gamma^{-1}\ln(\sqrt{b}/2\pi)| < t < t_c$ the initial-state probability is approximately given by
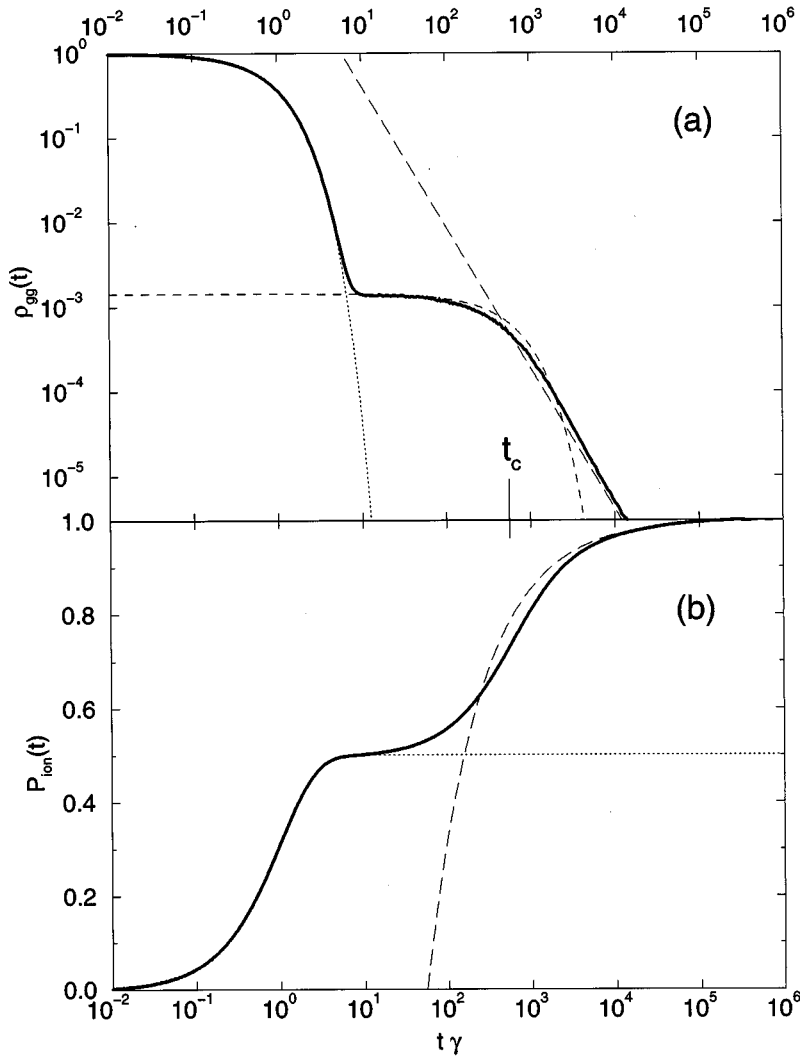
FIG. 5. Initial-state probability $\rho_{gg}(t)$ (a) and ionization probability $P_{\mathrm{ion}}(t)$ (b) as a function of interaction time t in units of $1/\gamma$ with $\gamma = 10^{-6}$ a.u. $= 4.13 \times 10^{10}$ s^{-1}, $\bar{\epsilon}/\gamma = 0.1$, and $b/\gamma = 80$. Various approximate time dependences are also indicated, namely, (a) $\rho_{gg}(t) = e^{-\gamma t}$ (dotted), Eq. (26) (short dashed), and Eq. (21) (long dashed); and (b) Eqs. (25) (dotted) and (24) (long dashed).

$$\rho_{gg}(t) = \frac{\sqrt{b}}{2\pi} e^{-\gamma \sqrt{b} t/(2\pi)}. \qquad (26)$$

For interaction times $t > t_c$ the ionization probability rises significantly, and finally saturates at the value of 1. This time evolution is described approximately by Eq. (24). At these large interaction times the initial-state probability decays according to Eq. (21).

In Fig. 6 continuum states well above the photoionization treshold are excited. Initially the ionization probability rises exponentially according to Eq. (25), and assumes the metastable value of φ/π. However, as in this case $\varphi \sim \pi$, already in this early stage of the excitation process the ionization probability rises to a value of almost 1. At long interaction times with $t > t_c$ the ionization probability rises to the final value of 1 according to Eq. (24). From Eqs. (11) and (B1) it is straightforward to show that for interaction times $|\gamma^{-1}\ln(\sqrt{b}/2\pi)| < t < t_c$ the decay of the initial state probability is approximately described by

$$\rho_{gg}(t) = \frac{\pi(2b+\gamma)^2}{8\varphi^2(2\bar{\epsilon})^{3/2}} \left(\frac{6}{7}\right)^{5/2} \exp\left\{ -t \frac{2\pi\gamma b(2b+\gamma)}{4\varphi(2\bar{\epsilon})^{3/2}} \left(\frac{6}{7}\right)^{5/2} \right\}. \qquad (27)$$

IV. SUMMARY AND CONCLUSIONS

The influence of phase fluctuations of a laser field on one-photon excitation of Rydberg and continuum states close to a photoionization threshold was investigated. This investigation concentrated on laser intensities which are small in comparison with the atomic unit of intensity. Therefore the interaction of the Rydberg electron with the fluctuating laser field takes place in a region extending a few Bohr radii around the atomic nucleus. The laser fluctuations tend to destroy the quantum coherence between probability amplitudes which are associated with repeated returns of the Rydberg electron to the core region where the electron-laser interaction is localized. As a consequence, the wave-packet dynamics of a Rydberg electron is affected significantly. In particular, at sufficiently long interaction times its dynamics is dominated by stochastic energy diffusion toward the photoionization threshold. The early stages of this diffusion process in which the Rydberg electron is energetically still well below threshold are governed by a $t^{-1/2}$ decay law of the initial state. At a critical time t_c [Eq. (16)], the Rydberg electron reaches the photoionization threshold by this diffusion process, and the ionization probability rises significantly. This threshold phenomenon is characterized by a $t^{-5/3}$ decay law of the initial state. The detailed analytical
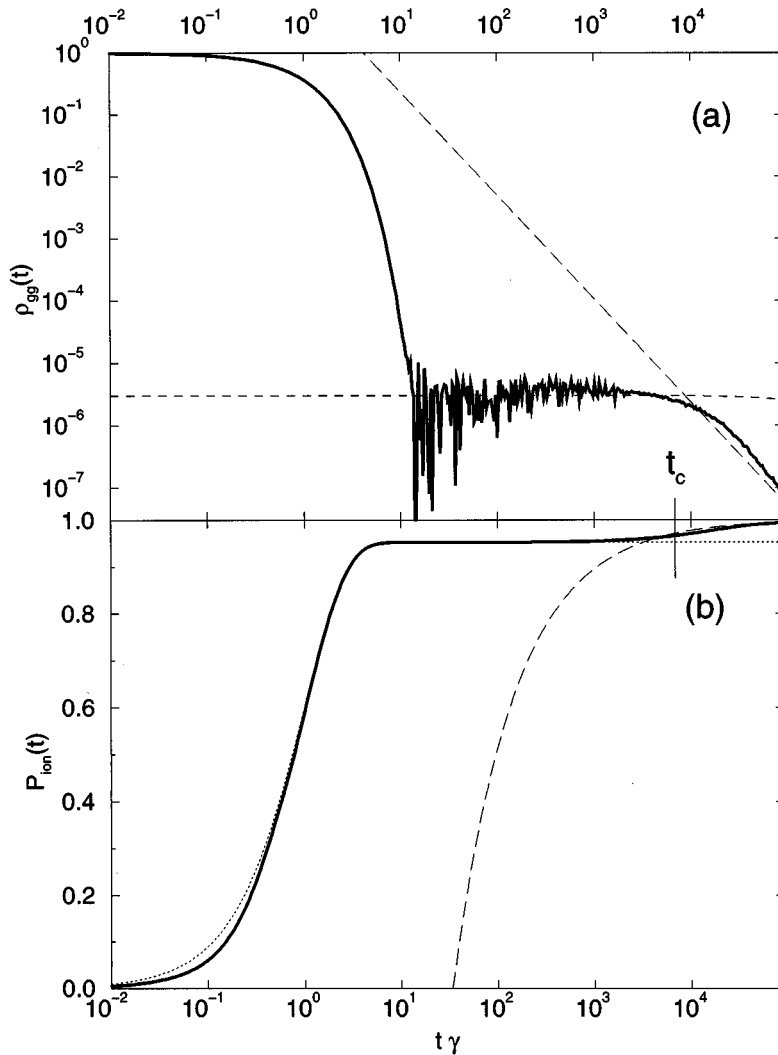
FIG. 6. Initial-state probability $\rho_{gg}(t)$ (a) and ionization probability $P_{\text{ion}}(t)$ (b) as a function of interaction time t in units of $1/\gamma$ with $\gamma = 10^{-6}$ a.u. $= 4.13 \times 10^{10}$ s^{-1}, $\bar{\epsilon}/\gamma = 10$, and $b/\gamma = 1$. Various approximate time dependences are also indicated, namely, (a) Eqs. (27) (short dashed) and (21) (long dashed); and (b) Eqs. (25) (dotted) and (24) (long dashed).

analysis of these nonexponential aspects has shown that t_c assumes its smallest value if Rydberg and continuum states are excited directly at threshold. The examples presented demonstrate that these diffusive threshold phenomena are observable as long as photon absorption from the excited Rydberg states is negligible.

Our investigation concentrated on effects arising from phase fluctuations of a single mode laser field which can be described by the PDM. Nowadays it is possible to control laser fluctuations experimentally [18]. Thus the presented diffusive threshold phenomena of Rydberg systems should be amenable to experimental observation. In the context of resonant one-photon excitation of two- and few-level systems by fluctuating laser fields, it is known [9] that in the limit of large laser bandwidths results obtained within the framework of the phase diffusion model also apply to other types of laser fluctuations with the same Lorentzian spectrum. This may be traced back to the fact that sufficiently large bandwidths imply correlation times of the laser fluctuations which are so short that relevant atom-field averages can be decorrelated. Within such a decorrelation approximation the dynamics of an excited atom is determined completely by the spectrum of the laser field, i.e., the lowest-order field correlation function. In view of these results it seems plausible that a similar conclusion also holds for the threshold phenomena discussed in this paper. However, this point

needs further investigation. Furthermore, effects of electron correlations which have to be described within the framework of quantum defect theory in a multichannel approximation might change the quantitative details of the nonexponential threshold phenomena. This aspect will be explored in subsequent work.

APPENDIX A

In this appendix explicit expressions are derived for the integral kernels $A_{ij}(z)$ of Eq. (10) in terms of contributions over all dressed states of the effective Hamiltonian $\bar{H}$. According to Eq. (11) these expressions are convenient for numerical evaluations of the density-matrix elements. Furthermore, they are starting points for the derivation of analytical results in various limiting cases.

With the help of Laplace transforms the kernels $A_{ij}(z)$ of Eq. (10) can be rewritten in the form $(i, j \in \{n, g\})$
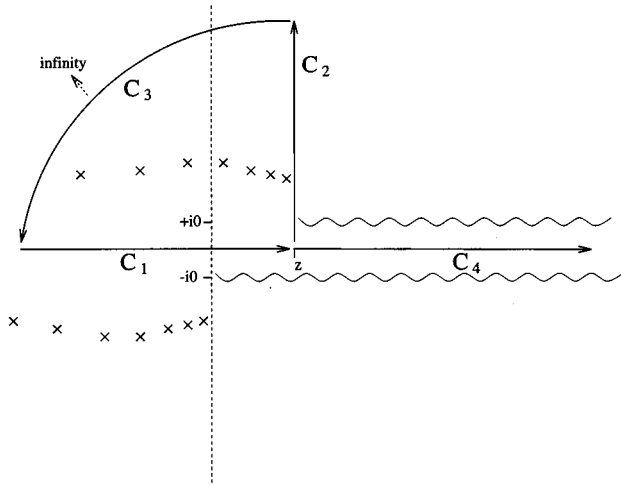
FIG. 7. Contours of integration in the complex z_1 plane.

$$A_{ij}(z) = \frac{1}{2\pi}\int_{-\infty}^{\infty} dz_1 a_{ig}(z_1+i0)[a_{jg}(z_1-z+i0)]^*,$$
$$(A1)$$

with

$$a_{ig}(z_1) = \langle i| \frac{i}{z_1+i0-\bar{H}} |g\rangle, \qquad (A2)$$

and $\bar{H}$ defined in Eq. (9). Therefore the complex amplitudes $a_{ig}(z)$ can be evaluated from the system of equations

$$(z_1+i0-\bar{\epsilon}+ib)a_{gg}(z_1-\omega) = -\langle g|\mathbf{d}\cdot\mathbf{E}_0|n\rangle^* a_{ng}(z_1)+i,$$
$$(A3)$$

$$(z_1+i0-\epsilon_n)a_{ng}(z_1) = -\langle n|\mathbf{d}\cdot\mathbf{E}_0|g\rangle a_{gg}(z_1-\omega),$$

in which $\bar{\epsilon} = \epsilon_g + \omega$ denotes the mean excited energy. These equations imply

$$a_{gg}(z_1-\omega) = i[z_1+i0-\bar{\epsilon}+ib-\Sigma(z_1)]^{-1},$$
$$(A4)$$

$$a_{ng}(z_1) = -[z_1+i0-\epsilon_n]^{-1}\langle n|\mathbf{d}\cdot\mathbf{E}_0|g\rangle a_{gg}(z_1-\omega).$$

The resonant part of the self-energy $\Sigma(z_1)$ of state $|g\rangle$ can be evaluated with the help of QDT. Thereby all effects arising from the infinitely many Rydberg and continuum states close to the photoionization threshold are taken into account properly. Within the framework of a one-channel approximation, its explicit form is given by Eq. (15). Evaluating Eq. (A1) with the help of contour integration in the complex z_1 plane $A_{ij}(z)$ can be represented as a sum over all dressed states of the effective Hamiltonian $\bar{H}$. For this purpose one has to take into account that $a_{gg}(z_1)$ has poles in the lower complex z_1 plane at the dressed energies $\widetilde{\epsilon}_n$ ($\text{Im}\,\widetilde{\epsilon}_n < 0$) which are determined by Eq. (14). This implies that $[a_{gg}(z_1-z)]^*$ has poles at $z_1 = z+\widetilde{\epsilon}_n^*$ in the upper complex z_1 plane. Thus, choosing for $0 < z \in \mathbf{R}$ the integration contours as shown in Fig. 7, and taking into account that the integral over curve C_3 vanishes, Eq. (13) is obtained with

$$C_2(z) = \frac{1}{2\pi}\int_z^{z+i\infty} dz_1[z_1-\bar{\epsilon}+i(\gamma/2+b)]^{-1}$$
$$\times [z_1-z-\bar{\epsilon}+i(\gamma/2-b)]^{-1},$$

$$C_4(z) = \frac{1}{2\pi}\int_z^{\infty} dz_1[z_1-\bar{\epsilon}+i(\gamma/2+b)]^{-1}$$
$$\times [z_1-z-\bar{\epsilon}+i(\gamma/2+b)]^{-1}. \qquad (A5)$$

Thereby the quantities $C_2(z)$ and $C_4(z)$ result from the contour integrations over curves C_2 and C_4 in Fig. 7. Explicit expressions for them in terms of logarithmic functions are given in Eq. (13). Note that the phases of these logarithmic functions have to be chosen in such a way that their arguments are continuous functions of z_1 along the relevant integration paths. For $0 > z \in \mathbf{R}$ the relation $A_{gg}(z) = [U(-z)]^*$ can be used, thus finally yielding Eq. (12).

Similar expressions may be derived for all other quantities $A_{ij}(z)$. In particular, it is found that

$$A_{\epsilon\epsilon'}(z) = V_{\epsilon\epsilon'}(z) + [V_{\epsilon'\epsilon}(-z)]^* \quad (z \in \mathbf{R}), \qquad (A6)$$

with

$$V_{\epsilon\epsilon'}(z) = \Theta(z)\langle\epsilon|\mathbf{d}\cdot\mathbf{E}_0|g\rangle\langle\epsilon'|\mathbf{d}\cdot\mathbf{E}_0|g\rangle^*$$
$$\times \left[\sum_{\text{Re}\,\widetilde{\epsilon}_n^* < 0} (z_1+i0-\epsilon)^{-1}(z_1-\bar{\epsilon}+ib \right.$$
$$-\Sigma(z_1+i0))^{-1}(z_1-z-i0-\epsilon')^{-1}$$
$$\times \left(1-\frac{d}{dz_1}\Sigma(z_1-i0) \right)^{-1}\bigg|_{z_1-z=\widetilde{\epsilon}_n^*}$$
$$\left. -D_2(z)+D_4(z) \right]. \qquad (A7)$$

The quantities $D_2(z)$ and $D_4(z)$ represent the relevant integrals over the curves C_2 and C_4 of Fig. 7. They are defined by

$$D_2(z) = \langle\epsilon|\mathbf{d}\cdot\mathbf{E}_0|g\rangle\langle\epsilon'|\mathbf{d}\cdot\mathbf{E}_0|g\rangle^* \frac{1}{2\pi}$$
$$\times \int_z^{z+i\infty} dz_1(z_1+i0-\epsilon)^{-1}(z_1-\bar{\epsilon}+i(b+\gamma/2))^{-1}$$
$$\times (z_1-z-i0-\epsilon')^{-1}(z_1-z-\bar{\epsilon}-i(b-\gamma/2))^{-1},$$

$$D_4(z) = \langle\epsilon|\mathbf{d}\cdot\mathbf{E}_0|g\rangle\langle\epsilon'|\mathbf{d}\cdot\mathbf{E}_0|g\rangle^* \frac{1}{2\pi}$$
$$\times \int_z^{\infty} dz_1(z_1+i0-\epsilon)^{-1}(z_1-\bar{\epsilon}+i(b+\gamma/2))^{-1}$$
$$\times (z_1-z-i0-\epsilon')^{-1}(z_1-z-\bar{\epsilon}-i(b-\gamma/2))^{-1}.$$
$$(A8)$$

Analogous to Eq. (13), these quantities can be expressed in a straightforward way by complex logarithmic functions. In

Eq. (A7), $\langle \epsilon | \mathbf{d} \cdot \mathbf{E}_0 | g \rangle$ and $\langle \epsilon' | \mathbf{d} \cdot \mathbf{E}_0 | g \rangle$ are energy-normalized dipole matrix elements. Replacing the energy-normalized continuum states $|\epsilon\rangle$ and $|\epsilon'\rangle$ by the normalized bound Rydberg states $|n\rangle$ and $|n'\rangle$, the corresponding kernel is obtained which determines the coherences of the Rydberg states.

APPENDIX B

In this appendix the behavior of $A_{gg}(z)$ in the complex z plane is investigated in a small neighborhood of its branch point at $z=0$. This determines the time evolution of the initial state probability $\rho_{gg}(t)$ in the long-time limit.

With the help of the sum rule of Eq. (C1) $A_{gg}(z)$ can be rewritten in the more convenient form $A_{gg}(z)=U(z)+[U(-z)]^*$ with

$$U(z)=\Theta(z)\left\{\frac{1}{2b}+I(z)-C_2(z)+C_4(z) - \frac{i}{4b\pi}\ln\frac{-\bar{\epsilon}-i(b+\gamma/2)}{-\bar{\epsilon}-i(b-\gamma/2)}\right\}, \quad (B1)$$

and with

$$I(z)=\frac{1}{2b}\sum_{\mathrm{Re}\,\tilde{\epsilon}_n^*<0}\left[1-\frac{d}{dz_1}\Sigma(z_1)\right]^{-1}\Bigg|_{z_1=\tilde{\epsilon}_n^*} \times \frac{-z-\tilde{\epsilon}_n^*+\bar{\epsilon}+ib+\Sigma(\tilde{\epsilon}_n^*+z)}{z+\tilde{\epsilon}_n^*-\bar{\epsilon}+ib-\Sigma(\tilde{\epsilon}_n^*+z)}. \quad (B2)$$

Using the one-channel approximation for the self-energy as given by Eq. (15), and neglecting ionization from the highly excited Rydberg states, i.e., putting $\beta=0$, Eq. (B2) yields

$$I(z)=-\frac{1}{2b}\sum_{\mathrm{Re}\,\tilde{\epsilon}_n^*<0}\left[1-\frac{d}{dz_1}\Sigma(z_1)\right]^{-1}\Bigg|_{z_1=\tilde{\epsilon}_n^*}$$
$$\times\frac{z+\tilde{\epsilon}_n^*-\bar{\epsilon}-i(b-\gamma/2)}{z+\tilde{\epsilon}_n^*-\bar{\epsilon}+i(b+\gamma/2)}$$
$$\times\frac{2\tan(\pi\tilde{\mu})[(z+\tilde{\epsilon}_n^*-\bar{\epsilon})^2+(b+\gamma/2)^2]}{2\tan(\pi\tilde{\mu})[(z+\tilde{\epsilon}_n^*-\bar{\epsilon})^2+(b^2+\gamma^2/4)]+i2b\gamma}, \quad (B3)$$

with

$$e^{2i\pi[-2(z+\tilde{\epsilon}_n^*)]^{-1/2}}[\tilde{\chi}^*(z+\tilde{\epsilon}_n^*)]^{-1}=e^{2i\pi\tilde{\mu}}. \quad (B4)$$

The laser-assisted scattering matrix $\tilde{\chi}(z)$ is given by

$$\tilde{\chi}(z)=e^{2i\pi\alpha}\left(1-i\frac{\gamma}{z-\bar{\epsilon}+i(b+\gamma/2)}\right). \quad (B5)$$

In particular, for $|z|\ll\sqrt{b^2+\gamma^2/4}$, one obtains

$$I(z)=-\sum_{\tilde{\epsilon}_n}\frac{\gamma}{2bT_{\tilde{\epsilon}_n^*}}\frac{1}{(\tilde{\epsilon}_n^*-\bar{\epsilon})^2+b^2+\gamma^2/4+i2b\gamma/[zT_{\tilde{\epsilon}_n^*}]}, \quad (B6)$$

with the classical orbit time $T_{\tilde{\epsilon}_n^*}=2\pi(-2\tilde{\epsilon}_n^*)^{-3/2}$ of the dressed energy $\tilde{\epsilon}_n^*$. In Eq. (B6) it was assumed that the density of states of the Coulomb problem is not modified significantly by the laser field, i.e., $T_{\tilde{\epsilon}_n^*}\gg\gamma/|(\tilde{\epsilon}_n^*-\bar{\epsilon}-i(b-\gamma/2))(\tilde{\epsilon}_n^*-\bar{\epsilon}-i(b+\gamma/2))|$. Furthermore, the quantity $\tilde{\mu}$ of Eq. (B4) was determined by linearizing the argument of the exponent, i.e., $2\pi\tilde{\mu}=T_{\tilde{\epsilon}_n^*}z$, and the approximation $\tan T_{\tilde{\epsilon}_n^*}z=T_{\tilde{\epsilon}_n^*}z+O((T_{\tilde{\epsilon}_n^*}z)^3)$ was used. As the summands of Eq. (B6) are smooth functions of $\tilde{\epsilon}_n^*$, Eq.(B6) can be evaluated approximately by replacing the summation by an integration. Thus it is found that

$$I(z)=-\frac{\gamma}{4b\pi(\bar{\epsilon}^2+b^2+\gamma^2/4)}\int_0^\infty d\nu\frac{\nu}{\Pi_{j=1}^4(\nu-\nu_j)}, \quad (B7)$$

with the characteristic roots $\nu_j=-Q_\pm/4\pm\sqrt{-R/2-S/4+T/Q_\pm}$ $(j=1,\ldots,4)$, and

$$Q_\pm=\pm 4\sqrt{R/2-S/4},$$

$$R=-2\,\mathrm{sgn}(q)\sqrt{|p|}\cos(\delta/3),$$

$$\cos(\delta)=\frac{|q|}{|p|^{3/2}},$$

$$q=\frac{\frac{2}{27}\bar{\epsilon}^3+\frac{b^2+\gamma^2/4}{12}\bar{\epsilon}+\frac{1}{8}\left(\frac{\gamma b}{\pi z}\right)^2(\bar{\epsilon}^2+b^2+\gamma^2/4)}{2(\bar{\epsilon}^2+b^2+\gamma^2/4)^3}, \quad (B8)$$

$$p=-\frac{\bar{\epsilon}^2+\frac{3}{4}(b^2+\gamma^2/4)}{9(\bar{\epsilon}^2+b^2+\gamma^2/4)^2},$$

$$S=\frac{\bar{\epsilon}}{\bar{\epsilon}^2+b^2+\gamma^2/4},$$

$$T=i\frac{b\gamma}{\pi z(\bar{\epsilon}^2+b^2+\gamma^2/4)}.$$

Performing the integration in Eq. (B7) with the help of the Mittag-Leffler expansion

$$\frac{\nu}{\Pi_{j=1}^4(\nu-\nu_j)}=\sum_{j=1}^4 A_j\left(1+\frac{\nu_j}{\nu-\nu_j}\right), \quad (B9)$$

with $A_j=1/\Pi_{j\neq l=1}^4(\nu_j-\nu_l)$, the final expression

$$I(z)=\frac{\gamma}{4b\pi(\bar{\epsilon}^2+b^2+\gamma^2/4)}\sum_{j=1}^4 A_j\nu_j\ln(-\nu_j) \quad (B10)$$

is obtained. Equation (B10) is valid under quite general conditions provided $|z| \ll \sqrt{b^2 + \gamma^2/4}$. It can be simplified further in the following limiting cases:

(1) If $|z| \ll 1/t_c$, with t_c as defined in Eq. (16),

$$I(z) = \frac{-2\pi}{12\sqrt{3}b^2}\left[\frac{b\gamma}{\pi(\bar{\epsilon}^2 + b^2 + \gamma^2/4)}\right]^{1/3} e^{-i\pi/3}z^{2/3}. \tag{B11}$$

(2) If $-\bar{\epsilon} \gg b$ and $1/t_c \ll |z| \ll \sqrt{b^2 + \gamma^2/4}$, Eq. (B10) yields

$$I(z) = -\frac{e^{-i\pi/4}}{8b^2}\sqrt{2b\gamma T_{\bar{\epsilon}}}z^{1/2}. \tag{B12}$$

Inserting these relations into Eq. (B1) the asymptotic expressions of Eqs. (17) and (19) are obtained.

APPENDIX C

In this appendix the useful sum rule

$$1 = \sum_{\mathrm{Re}\,\tilde{\epsilon}_n < 0}\left[1 - \frac{d}{dz_1}\Sigma(z_1)\right]^{-1}\Bigg|_{z_1 = \tilde{\epsilon}_n} - \frac{i}{2\pi}\ln\frac{-\bar{\epsilon} + i(b + \gamma/2)}{-\bar{\epsilon} + i(b - \gamma/2)} \tag{C1}$$

is derived.

For this purpose, let us consider the integral

$$J_C = \frac{1}{2\pi}\int_C dz\, i[z - \bar{\epsilon} + ib - \Sigma(z)]^{-1} \tag{C2}$$

along the curves C in the complex z plane depicted in Fig. 8. The only poles of the integrand of Eq. (C2) are located at the dressed energies $z = \tilde{\epsilon}_n$ in the lower half of the complex z plane and at $z = \infty$. Furthermore, the integrand has a branch cut extending along the positive real z axis. It is obvious from Fig. 8 that

$$J_{C_1} - J_{C_2} = (J_{C_5} - J_{C_4} - J_{C_2}) + (J_{C_4} - J_{C_3}). \tag{C3}$$

The left-hand side of this equation is a contour integral which encircles the pole at $z = \infty$ in the counterclockwise sense, thus yielding
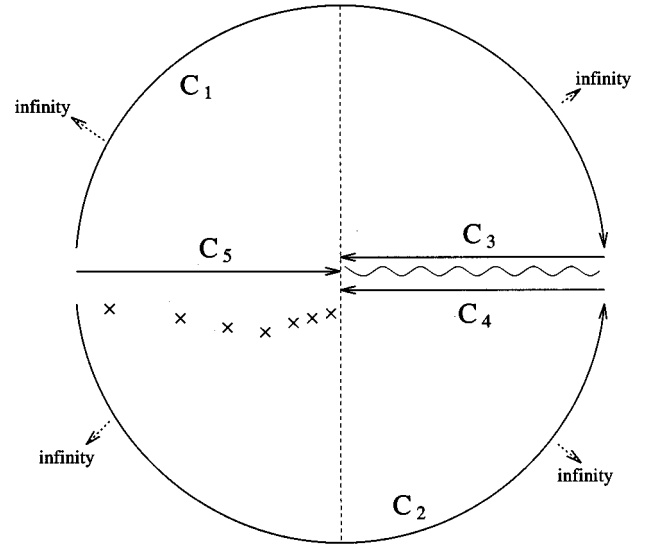
$$J_{C_1} - J_{C_2} = 1. \tag{C4}$$

FIG. 8. Contours of integration in the complex z plane.

The presence of the poles at $z = \tilde{\epsilon}_n$ in the lower half of the complex z plane implies

$$J_{C_5} - J_{C_4} - J_{C_2} = \sum_{\tilde{\epsilon}_n}\left[1 - \frac{d}{dz}\Sigma(z)\right]^{-1}\Bigg|_{z = \tilde{\epsilon}_n}. \tag{C5}$$

Using Eq. (15) for the self-energy in the one-channel approximation, the remaining contour integrations can be performed easily, i.e.,

$$J_{C_4} - J_{C_3} = \frac{1}{2\pi}\int_0^\infty dz\, i\{[z - \bar{\epsilon} + i(b + \gamma/2)]^{-1}$$
$$- [z - \bar{\epsilon} + i(b - \gamma/2)]^{-1}\}$$
$$= -\frac{i}{2\pi}\ln\frac{-\bar{\epsilon} + i(b + \gamma/2)}{-\bar{\epsilon} + i(b - \gamma/2)}. \tag{C6}$$

Using Eqs. (C4), (C5), and (C6) finally the sum rule of Eq. (C1) is obtained.

---

[1] U. Weiss, *Quantum Dissipative Systems*, Series in Modern Condensed Matter Physics Vol. 2 (World Scientific, Singapore, 1993).

[2] P. Zoller, Phys. Rev. A **20**, 1019 (1979); S. N. Dixit, P. Zoller, and P. Lambropoulos, *ibid.* **21**, 1289 (1980); R. Walser, H. Ritsch, P. Zoller, and J. Cooper, *ibid.* **45**, 468 (1992).

[3] A. Giusti-Suzor and P. Zoller, Phys. Rev. A **36**, 5178 (1987).

[4] M. J. Seaton, Rep. Prog. Phys. **46**, 167 (1983).

[5] R. Blümel, R. Graham, L. Sirko, U. Smilansky, H. Walter, and K. Yamada, Phys. Rev. Lett. **62**, 341 (1989).

[6] U. Fano and A. R. P. Rau, *Atomic Collision and Spectra* (Academic, New York, 1986).

[7] H. Haken, in *Handbuch der Physik*, edited by S. Flügge (Springer, New York, 1970), Vol. XXV/2c.

[8] G. Alber and P. Zoller, Phys. Rev. Lett. . **199**, 231 (1991).

[9] G. S. Agarwal, Phys. Rev. Lett. **37**, 1383 (1976); Phys. Rev. A **18**, 1490 (1978).

[10] V. B. Braginsky and F. Ya. Khalili, *Quantum Measurement* (Cambridge University Press, Cambridge, 1992).

[11] G. Alber and P. Zoller, Phys. Rev. A **37**, 377 (1988).

[12] L. D. Landau and E. M. Lifshitz, *The Classical Theory of Fields* (Pergamon, Oxford, 1975), p. 181ff.

[13] P. E. Klöden and E. Platen, *Numerical Solution of Stochastic Differential Equations* (Springer, Berlin, 1992).

[14] B. R. Mollow, Phys. Rev. A **12**, 1919 (1975).

[15] M. L. Goldberger and K. M. Watson, *Collision Theory* (Wiley, New York, 1964).

[16] *Handbook of Mathematical Functions*, edited by M. Abramowitz and I. Stegun, Natl. Bur. Stand. Appl. Math. Ser. No. 55 (U.S. GPO, Washington, DC, 1964).

[17] B. Misra and E. C. Sudarshan (N.Y.), J. Math. Phys. (N.Y.) **18**, 756 (1977).

[18] G. Vemuri, M. H. Anderson, J. Cooper, and S. J. Smith, Phys. Rev. A **44**, 7635 (1991); M. H. Anderson, G. Vemuri, J. Cooper, P. Zoller, and S. J. Smith, *ibid.* **47**, 3202 (1993).